Available online at www.sciencedirect.com
ScienceDirect
International Journal of Mass Spectrometry 257 (2006) 41–49
International Journal of Mass Spectrometry
www.elsevier.com/locate/ijms

Mass spectrometric determination of ternary interaction parameters of liquid Cu–In–Sn alloy

A. Popovic [a,*], L. Bencze [b]

[a] *Jozef Stefan Institute, Jamova 39, SLO-1000 Ljubljana, Slovenia*
[b] *Eötvös Loránd University, Department of Physical Chemistry, H-1117 Budapest, Pázmány Péter sétány 1/A, Hungary*

Received 5 May 2006; received in revised form 15 June 2006; accepted 16 June 2006
Available online 24 July 2006

Abstract

The vaporisation of a liquid Cu–In–Sn system has been investigated between 1273 and 1473 K using Knudsen effusion mass spectrometry (KEMS) and the data obtained fitted to a Redlich–Kister sub-regular solution model. We examined 23 different compositions at four fixed indium concentrations: $x_{In} = 0.20, 0.25, 0.29, 0.30$ and 0.40 and evaluate the thermodynamic activities of all three components, not by applying the standard KEMS pressure calibration procedure, but from the measured ion intensity ratios of Cu^+ to Sn^+ using a recently published mathematical regression technique. The intermediate data obtained directly from the regression technique are the Redlich–Kister ternary L-parameters that are, as a function of temperature, as follows:

$$L^0 = (-59473 \pm 7057) + (726.8 \pm 42.3)\cdot T - (89.0 \pm 5.1)\cdot T\cdot\ln(T);$$
$$L^1 = (156840 \pm 5.2\text{E}-9) - (80 \pm 3.3\text{E}-11)\cdot T - (5.57\text{E}-11 \pm 4\text{E}-12)\cdot T\cdot\ln(T);$$
$$L^2 = (-137168 \pm 8819) + (592.4 \pm 52.9)\cdot T - (70.6 \pm 6.4)\cdot T\cdot\ln(T).$$

By using these values together with binary parameters taken from the literature, we were able to calculate several other thermodynamic functions of mixing. In particular, the partial heat of mixing of indium and its activity, which we evaluated and compared with the measured values along the Cu/Sn = 1 isopleths. We obtained a good agreement between the calculated and measured values for partial heats while in the case of activity a good agreement between the two data sets is limited to a lower mole fraction of indium.

Keywords: Ternary interaction parameters; Knudsen cell; Lead free solder; Alloys

1. Introduction

The search for a replacement for tin–lead solder in the electronic industries is of increasing importance. According to the European Directive covering "Waste from Electrical and Electronic Equipment" (WEEE Directive from 2000) there will be a complete ban on the use of lead solders after January 2008. There is a general agreement that there will be no single drop-in replacement for lead–tin solders and that the future choice of solder material will be application-dependent. A number of possible replacements are under investigation including binary, ternary and even quaternary alloy systems composed of Sn, Cu, Ag, In, Zn, Ni, Au and Pd. Indium is included here due to its low melting point while palladium, gold, copper and nickel also represent possible substrate materials. Among the options available, many regard the Ag–In–Sn and Cu–In–Sn ternary alloy systems as candidates for suitable replacements for lead-tin solder, the latter being of interest in the present work.

All binary combinations of the elements mentioned above have been studied using different methods to obtain their activities and other thermodynamic quantities of mixing. We can use this data to make a critical assessment of a particular binary system. As a result, a set of thermodynamic parameters is available to describe the phase equilibrium of binary systems. However, for ternary and quaternary systems the greater number

* Corresponding author. Tel.: +386 1 4773490; fax: +386 1 251985.
E-mail address: arkadij.popovic@ijs.si (A. Popovic).

1387-3806/$ – see front matter © 2006 Elsevier B.V. All rights reserved.
doi:10.1016/j.ijms.2006.06.010

of solid phases makes the situation complex and less experimental activity data and phase diagram information exists. In general, the ternary interaction parameters are obtained from various experimental data including a phase diagram, chemical potential, thermodynamic activity and enthalpy data by trial and error or better still mathematically using the CALPHAD method [1–3]. In 2001 Miki et al. [4] were able to show, that by using the Redlich–Kister sub-regular solution model they could obtain the ternary interaction parameters from direct mass spectrometric measurements. More recently, Schmidt and Tomiska [5] independently developed a similar mass spectrometric method by using thermodynamic adoptive parameters (TAP) to describe the individual phases present. In our work, we use Miki's mass spectrometric method to determine ternary interaction parameters of a Cu–In–Sn liquid system.

2. Experimental

For our experiments, we used a Nier type mass spectrometer in combination with a Knudsen cell. Although, the experimental technique is described in full elsewhere [6], in brief, a typical experiment consists of heating the sample in the cell to a specific temperature. The sample vapours, effuse through a small cell orifice, into the ionisation chamber where they are ionised prior to being separated by their masses before being detected and their abundances measured using an electron multiplier operated in the counting mode at −3.0 kV feed (for a detailed description of the experimental setup see Ref. [7]).

In such an arrangement, above the condensed sample, it is possible to obtain the equilibrium vapour pressure (p_j) of the molecular species 'j', within the Knudsen cell, using Eq. [1]

$$p_j = \frac{\text{Cons} \cdot T}{\sigma_j} \sum_k \frac{I_{jk}^+}{\eta_{jk} \cdot \gamma_{jk}} \tag{1}$$

where I_{jk}^+ is the intensity of ion k formed from the molecular species j; T the absolute temperature of the Knudsen cell; Cons the general sensitivity constant of the particular instrument; σ_j the ionisation cross section of the molecular species j at the measured ionising electron energy; η_{jk} the isotope correction factor of ion k; γ_{jk} is the multiplier efficiency for ion k.

We can also obtain the variation in the vapour pressure ratio of the two given species with temperature by measuring their ion current ratio variation without explicit knowledge of the values of the parameters in Eq. (1). This important feature of Knudsen Cell Mass Spectrometry (KCMS) makes it an effective technique for measuring the activities and thermodynamic quantities of binary systems [8].

3. Thermodynamics and Redlich–Kister sub-regular solution model

The Gibbs energy of a binary liquid or solid mixture can be described as random mixtures of elements A and B by a sub regular-solution type model (Eq. (2)):

$$G = X_A G_A^\circ + X_B G_B^\circ + RT(X_A \ln X_A + X_B \ln X_B) + X_A X_B \left(\sum_{i=0}^{i} L_i (X_A - X_B)^i \right) \tag{2}$$

where X_A and X_B are the mole fractions, and G_A° and G_B° are the reference state of both elements. The first two terms represent the mechanical mixture of the elements, the third the entropy of mixing (ideal mixing) and the fourth the excess Gibbs energy. This excess Gibbs energy is characterised by values of L's called binary interaction parameters, which are already determined for the majority of liquid binary systems. Binary parameters can further be used to obtain the excess Gibbs energy (G^E) of a ternary system after the method of Muggianu [9], as follows: Eq. (3).

$$G^E = X_A X_B \sum_{i=0}^{n_{AB}} L_i^{AB} (X_A - X_B)^i + X_A X_C \sum_{i=0}^{n_{AC}} L_i^{AC} (X_A - X_C)^i + X_B X_C \sum_{i=0}^{n_{BC}} L_i^{BC} (X_B - X_C)^i + X_A X_B X_C [L_0^{ABC}(X_A) + L_1^{ABC}(X_B) + L_2^{ABC}(X_C)] \tag{3}$$

The last term, defined by L^{ABC} includes the contribution of the ternary interaction to the Gibbs energy.

In the work of Miki et al. [4] it is assumed that all three ternary parameters are equal in which case the last term of Eq. (3) reduces to $L^{ABC}(X_A X_B X_C)$. In our case, no such simplification is possible making the mathematical analysis of the experimental data increasingly complex.

For the ternary system investigated in this work we substitute the notation A, B and C with Cu, In and Sn, respectively. By partial differentiation, we obtain the excess partial chemical potential of Cu and Sn as (Eqs. (4) and (5)):

$$\mu_{Cu}^E = G^E - X_{In} \left(\frac{\partial G^E}{\partial X_{In}} \right)_{Cu} + (1 - X_{Cu}) \left(\frac{\partial G^E}{\partial X_{Cu}} \right)_{In} \tag{4}$$

$$\mu_{Sn}^E = G^E - X_{Cu} \left(\frac{\partial G^E}{\partial X_{Cu}} \right)_{In} - X_{In} \left(\frac{\partial G^E}{\partial X_{In}} \right)_{Cu} \tag{5}$$

and therefore:

$$\mu_{Cu}^E - \mu_{Sn}^E = RT \ln \left(\frac{\gamma_{Cu}}{\gamma_{Sn}} \right) = \left(\frac{\partial G^E}{\partial X_{Cu}} \right)_{ln} \tag{6}$$

The excess Gibbs energy Eq. (3) for a Cu–In–Sn ternary system, using the necessary number of binary and ternary L parameters then becomes Eq. (7):

$$\begin{aligned} G^E = {} & X_{Cu} X_{In} [L_{Cu-In}^0 + L_{Cu-In}^1 (X_{Cu} - X_{In}) + L_{Cu-In}^2 (X_{Cu} - X_{In})^2] + X_{Cu}(1 - X_{Cu} - X_{In}) \\ & \times [L_{Cu-Sn}^0 + L_{Cu-Sn}^1 (2X_{Cu} - 1 + X_{In}) + L_{Cu-Sn}^2 (2X_{Cu} - 1 + X_{In})^2] + X_{In}(1 - X_{Cu} - X_{In}) \\ & \times [L_{In-Sn}^0 + L_{In-Sn}^1 (2X_{In} - 1 + X_{Cu})] \end{aligned}$$

$$+ X_{Cu}X_{In}(1 - X_{Cu} - X_{In})[L^0_{Cu-In-Sn}X_{Cu} + L^1_{Cu-In-Sn}X_{In} + L^2_{Cu-In-Sn}(1 - X_{Cu} - X_{In})] \quad (7)$$

Here, n_{AB} for the In–Sn binary is 2 (Eq. (18)), since only two binary parameters describe the In–Sn system whereas for Cu–In and Cu–Sn $n = 3$ (Eqs. (16) and (17)). The mole fraction of Sn in Eq. (7) is replaced with $X_{Sn} = 1 - X_{Cu} - X_{In}$.

$$\begin{bmatrix} 1 & ((2X_{Sn} - X_{Cu}) \cdot X_{Cu}X_{In})_1 & ((X_{Sn} - X_{Cu}) \cdot X^2_{In})_1 & ((X_{Sn} - 2X_{Cu}) \cdot X_{Sn}X_{In})_1 \\ 1 & ((2X_{Sn} - X_{Cu}) \cdot X_{Cu}X_{In})_2 & ((X_{Sn} - X_{Cu}) \cdot X^2_{In})_2 & ((X_{Sn} - 2X_{Cu}) \cdot X_{Sn}X_{In})_2 \\ . & . & . & . \\ 1 & ((2X_{Sn} - X_{Cu}) \cdot X_{Cu}X_{In})_n & ((X_{Sn} - X_{Cu}) \cdot X^2_{In})_n & ((X_{Sn} - 2X_{Cu}) \cdot X_{Sn}X_{In})_n \end{bmatrix} \begin{bmatrix} -C \\ L^0_{Cu-In-Sn} \\ L^1_{Cu-In-Sn} \\ L^2_{Cu-In-Sn} \end{bmatrix} = \begin{bmatrix} Y\text{summa}_1 \\ Y\text{summa}_2 \\ . \\ Y\text{summa}_n \end{bmatrix}$$

Eq. (6) shows that the partial derivative of G^E is needed with respect to X_{Cu} at constant X_{In}. After rearrangement, the resulting $(\partial G^E/\partial X_{Cu})/X_{In}$ can be expressed as Eq. (8):

$$\left(\frac{\partial G^E}{\partial X_{Cu}}\right)_{In} = L^0_{Cu-In-Sn}(2X_{Sn} - X_{Cu})X_{Cu}X_{In} + L^1_{Cu-In-Sn}(X_{Sn} - X_{Cu})(X_{In})^2 + L^2_{Cu-In-Sn}(X_{Sn} - 2X_{Cu})X_{Sn}X_{In} - Y \quad (8)$$

where

$$\begin{aligned} Y = -\{&X_{In}[L^0_{Cu-In} + L^1_{Cu-In}(X_{Cu} - X_{In}) + L^2_{Cu-In}(X_{Cu} - X_{In})^2] + X_{Cu}X_{In}[L^1_{Cu-In} + 2L^2_{Cu-In}(X_{Cu} - X_{In})] + (1 - X_{In} - 2X_{Cu}) \\ &\times [L^0_{Cu-Sn} + L^1_{Cu-Sn}(2X_{Cu} - 1 + X_{In}) + L^2_{Cu-Sn}(2X_{Cu} - 1 + X_{In})^2] + X_{Cu}(1 - X_{In} - X_{Cu}) \\ &\times [2L^1_{Cu-Sn} + 4L^2_{Cu-Sn}(2X_{Cu} - 1 + X_{In})] \\ &- X_{In}[L^0_{In-Sn} + L^1_{In-Sn}(3X_{In} - 2 + 2X_{In})] \end{aligned}$$

From the basic KEMS, using Eq. (1), it can be shown that:

$$\left(\frac{\partial G^E}{\partial X_{Cu}}\right)_{In} = R \cdot T \cdot \ln\left(\frac{\gamma_{Cu}}{\gamma_{Sn}}\right) = R \cdot T \cdot \ln\left(\frac{I^+_{Cu} \cdot X_{Sn}}{I^+_{Sn} \cdot X_{Cu}}\right) + C \quad (9)$$

where γ represents the activity coefficient of a given element and C is an experimental constant (does not depend on composition). The equation includes the parameters described in Eq. (1) and the standard Gibbs free energies of evaporation of the pure measured elements.

Introducing the notations

$$YY \equiv R \cdot T \cdot \ln\left(\frac{I^+_{Cu}X_{Sn}}{I^+_{Sn}X_{Sn}}\right) \quad (10)$$

and

$$Y\text{summa} \equiv Y + YY \quad (11)$$

it follows that:

$$Y\text{summa} = -C + L^0_{Cu-In-Sn}(2X_{Sn} - X_{Cu})X_{Cu}X_{In} + L^1_{Cu-In-Sn}(X_{Sn} - X_{Cu})(X_{In})^2 + L^2_{Cu-In-Sn}(X_{Sn} - 2X_{Cu})X_{Sn}X_{In} \quad (12)$$

where $X_{Cu} + X_{In} + X_{Cu} = 1$.

We obtain the parameters by solving a set of linear equations:

where 'n' is the number of the measured compositions and since 23 compositions were measured, the solution to the linear equations must be replaced with a regression problem.

4. Sample preparation and measuring procedure

Known quantities of metals purchased from SIGMA–ALDRICH (500 mg of total mass) were collected in a small graphite cup and placed inside a vertical quartz tube into which a 7% hydrogen in argon mixture was fed during the melting process at 800 °C for 2 h. The use of a reductive atmosphere during melting was necessary to expel any traces of oxygen present in the metals as a surface or bulk impurity. When using pure (99.99%) argon as a protective gas an intense signal for the In_2O^+ ion appears in the mass spectrum. In_2O is formed according to the following reaction [10]:

$$In_2O_3(s) + 4In(liquid) = 3In_2O(g)$$

The high volatility of In_2O enhances the loss of indium during its pressure determination (mass loss experiments). Nevertheless, in spite of using the reductive gas for sample preparation it was not possible to avoid the appearance of traces of the In_2O^+ ion in the mass spectrum. Typically, the sample was loaded in a cylindrical alumina cell (10 mm × 10 mm Ø) with a channel type orifice of 0.55 mm diameter. The cell was inserted in the evaporator [7] and evacuated to high vacuum. The cell was then heated to 1473 K at 20 K/min. The abundance of In_2O^+ ion was monitored during the temperature gradient. At 1473 K the ion abundance rapidly decreased to below 500 counts/s. A typical mass loss (loss of mostly indium via In_2O) during heating was less than 0.5 mg. At 1473 K the intensities of the $^{63}Cu^+$ and $^{120}Sn^+$ ions were measured at 10° intervals down to 1273 K. The raw data for a typical run (sample no. 17, see Table 3) are depicted in Table 1.

A second type of experiment involving the direct indium activity measurement was performed using the standard Knudsen effusion mass loss rate method [6]. In this case, the method involves measuring the mass loss rate of the alloy sample relative to the mass loss rate of pure indium at an equivalent temperature. We performed these measurements at 1173 K. To accomplish this, the cell was loaded with known amounts (1000 mg) of the alloy and/or pure indium, evacuated and heated to 1173 K at

Table 1
Ion currents of ^{63}Cu and ^{120}Sn in variation of temperature for $Cu_{0.304}$–$In_{0.3}$–$Sn_{0.396}$ alloy

T (K)	$^{63}I^{+}_{Cu}$ (Hz)	$^{120}I^{+}_{Sn}$ (Hz)	$\ln\left(\frac{I^{+}_{Cu}}{I^{+}_{Sn}}\cdot\frac{X_{Sn}}{X_{Cu}}\right)$
1485	12900	44000	−0.9626
1475	12300	41800	−0.9589
1463	10000	33000	−0.9295
1453	7900	28000	−1.0010
1446	7300	24300	−0.9382
1439	5700	20600	−1.0204
1430	4800	17700	−1.0406
1415	3700	13400	−1.0225
1402	2850	11000	−1.0862
1390	2500	9600	−1.0811
1371	1704	6662	−1.0991
1355	1236	5260	−1.1839
1348	1111	4633	−1.1636
1332	750	3228	−1.1952
1326	742	3188	−1.1934
1310	577	2567	−1.2283
1297	418	1963	−1.2824

20 K/min. After an appropriate time the cell was cooled to room temperature and weighed. The activity of indium was then determined using Eq. (13):

$$a_{In} = \frac{\Delta m_{sample}/\Delta t_{sample}}{\Delta m_{In(pure)}/\Delta t_{In(pure)}} \quad (13)$$

where Δm and Δt represent the mass loss and the time of evaporation, respectively. Several runs were performed for each composition as shown in Table 2 . This simple relationship implies that activity can be determined with reasonable reliability since the systematic error can result only from the enhanced evaporation of indium *via* the loss of $In_2O(g)$ and a small change in composition during evaporation. A typical mass loss from an initial 1000 mg of sample is only 0.5–4 mg, and means that no composition correction is required. We also assume that at 1173 K the contributions of Cu and Sn to the total mass loss are negligible.

5. Results and discussion

In an early stage in our investigation we supposed that, as in the work of Miki et al. [4] (Ag–In–Sn system), only one ternary parameter is sufficient to characterise the Cu–In–Sn liquid system. Therefore we followed strictly Miki's [4] derivation. In addition, we took the decision to measure the Cu^+ and Sn^+ ion intensities and not that of In^+ due to the high indium vapour pressure. According to Miki's original procedure, the ternary parameter was represented by the slope of Ysumma versus $X_{Sn}\cdot(-X_{Ag}+X_{In})$. It should be noted that our sample compositions were selected so that the maximum possible range of the X-axis $[X_{In}\cdot(X_{Sn}-X_{Cu})]$ was achieved. At the same time the mole fraction of indium had to be kept low to prevent the excessive mass loss of indium at higher temperatures and to stay in the effusion regime [6]. The result was that we succeeded in measuring the X-axis within $-0.2 \le X_{In}\cdot(X_{Sn}-X_{Cu}) \ge 0.2$. Fig. 1 show the measured compositions in the ternary composi-

Table 2
Experimental data for indium activity determination of Cu–In–Sn alloys using Knudsen effusion (mass loss) method

Composition (Sn/Cu = 1)	Evaporation time (h)	Mass loss (mg)	Mass loss rate (mg/h)	Activity
$X_{In}=0.05$	41.50	1.92	0.0463	0.103[b]
	45.92	1.34	0.0292	0.065
	43.08	0.96	0.0223	0.049
	23.28	0.57	0.0245	0.054
	66.08	1.78	0.0269	0.060
Average				0.057
$X_{In}=0.1$	45.83	2.49	0.0543	0.12[b]
	21.50	1.00	0.0465	0.10
	42.00	2.06	0.0490	0.11
Average				0.11
$X_{In}=0.15$	42.97	3.31	0.0770	0.17
	45.47	3.09	0.0680	0.15
	43.03	2.87	0.0667	0.15
Average				0.16
$X_{In}=0.2$	23.92	2.51	0.1049	0.23
	22.42	2.41	0.1075	0.24
Average				0.24
$X_{In}=0.3$	17.72	3.30	0.1863	0.41
	18.83	3.05	0.1619	0.36
	21.38	3.50	0.1637	0.36
Average				0.38
$X_{In}=0.4$	19.00	3.41	0.1795	0.40
	19.00	3.45	0.1816	0.40
	18.00	3.36	0.1867	0.41
Average				0.48
$X_{In}=0.5$	11.72	2.61	0.2228	0.49
	11.50	2.57	0.2235	0.50
	10.90	2.26	0.2073	0.46
Average				0.48
$X_{In}=0.6$	10.17	2.99	0.2941	0.65
	10.17	2.93	0.2882	0.64
	10.17	2.97	0.2921	0.65
Average				0.65
$X_{In}=0.7$	10.17	3.21	0.3157	0.70
	10.17	3.47	0.3413	0.76
	10.17	3.47	0.3413	0.76
Average				0.74
$X_{In}=0.8$	10.17	3.92	0.3856	0.86
	10.17	4.13	0.4062	0.90
	10.17	3.81	0.3748	0.83
	10.17	4.80	0.4721	1.05[b]
	10.17	4.00	0.3934	0.87
Average				0.87
Pure In	10.17	4.52	0.4446	0.99
	10.17	4.53	0.4456	0.99
	10.17	4.62	0.4544	1.01
	10.17	4.45	0.4377	0.97
	10.17	4.77	0.4692	1.04
Average			0.4503[a]	
$X_{In}=0.4$	10.17	2.15	0.2115	0.47
	10.17	2.06	0.2026	0.45

Table 2 (*Continued*)

Composition (Sn/Cu = 1)	Evaporation time (h)	Mass loss (mg)	Mass loss rate (mg/h)	Activity
	10.17	2.42	0.2380	0.53[b]
	10.17	1.50	0.1475	0.33[b]
	10.17	1.96	0.1928	0.43
	10.17	1.89	0.1859	0.41
	10.17	1.88	0.1849	0.41
Average				0.43
$X_{In} = 0.5$	10.17	2.67	0.2626	0.58
	10.17	2.27	0.2233	0.50
	10.17	2.28	0.2243	0.50
	10.17	2.56	0.2518	0.56
	10.17	2.66	0.2616	0.58
	10.17	2.50	0.2458	0.55
Average				0.54
$X_{In} = 0.6$	10.17	3.00	0.2951	0.66
	10.17	2.98	0.2931	0.65
	10.17	2.89	0.2843	0.63
	10.17	2.79	0.2744	0.61
Average				0.64
$X_{In} = 0.7$	10.17	3.61	0.3551	0.79
	10.17	3.53	0.3472	0.77
	10.17	3.65	0.3590	0.80
Average				0.79

[a] Average mass loss of the pure indium.
[b] Not included in averaging.

Table 3
The parameters of $YY \equiv RT \ln(I_{Cu}X_{Sn}/I_{Sn}X_{Cu}) = (\alpha/T) + \beta$ equation for all the measured compositions

$$\ln\left(\frac{I^+_{Cu}}{I^+_{Sn}} \cdot \frac{X_{Sn}}{X_{Cu}}\right) = \left(\frac{\alpha}{T}\right) + \beta$$

Sample	X_{Cu}	X_{Sn}	X_{In}	α	β
1	0.1	0.6	0.30	−2448.6	0.51
2	0.5	0.1	0.40	−5246.6	2.69
3	0.533	0.267	0.20	−4859.0	2.54
4	0.267	0.533	0.20	−2019.3	0.26
5	0.2	0.4	0.40	−3687.3	1.53
6	0.4	0.2	0.40	−3942.3	1.80
7	0.3	0.3	0.40	−1794.6	0.25
8	0.15	0.45	0.40	−2508.4	0.80
9	0.45	0.15	0.40	−5215.9	2.73
10	0.1	0.5	0.40	−2525.3	0.65
11	0.583	0.117	0.30	−4942.5	2.65
12	0.16	0.64	0.20	−3827.0	1.48
13	0.64	0.16	0.20	−3760.0	2.05
14	0.1	0.6	0.30	−2448.4	0.51
15	0.6	0.1	0.30	−3528.5	1.77
16	0.631	0.079	0.29	−2289.0	1.01
17	0.304	0.396	0.30	−3418.6	1.37
18	0.396	0.304	0.30	−3848.5	1.74
19	0.64	0.16	0.20	−3309.6	1.77
20	0.436	0.364	0.20	−3965.3	1.71
21	0.4	0.4	0.20	−3097.3	1.11
22	0.625	0.125	0.25	−4966.4	2.89
23	0.127	0.573	0.30	−2270.1	0.45

The values behind ± are the standard deviations of the statistical error.

tion diagram while Table 3 gives the temperature dependence of $YY \equiv RT \ln(I^+_{Cu}X_{Sn}/I^+_{Sn}X_{Sn})$ in the form of $(\alpha/T) + \beta$ for each measured composition.

Fig. 2 represents the values of Y, YY and Ysumma as a function of $X_{In}\cdot(X_{Sn} - X_{Cu})$. We note here that Y is the derivative of the binary part of the total G^E with respect to X_{Cu} at constant X_{In} : $(\partial G^E/\partial X_{Cu})_{X_{In}}$ which is independent of our measurements but is a function of the binary parameters taken from the literature. In contrast, we obtain YY directly from our measurements. We also observe in Fig. 2 that both Y versus $X_{In}\cdot(X_{Sn} - X_{Cu})$ and YY versus $X_{In}\cdot(X_{Sn} - X_{Cu})$ are more scattered than Ysumma versus $X_{In}\cdot(X_{Sn} - X_{Cu})$. In an ideal case

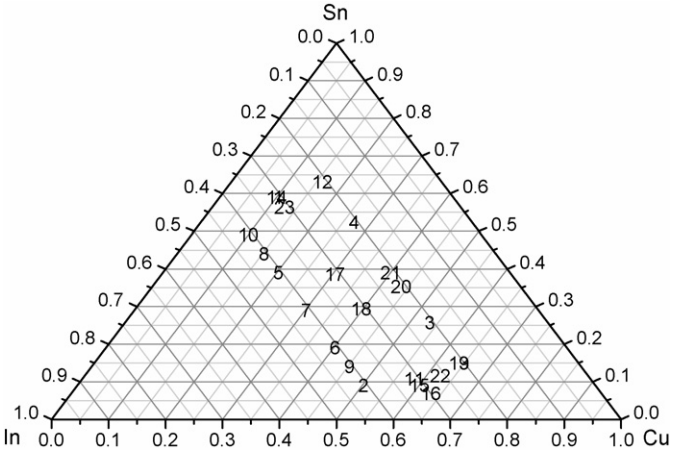

Fig. 1. Compositions of the measured samples.

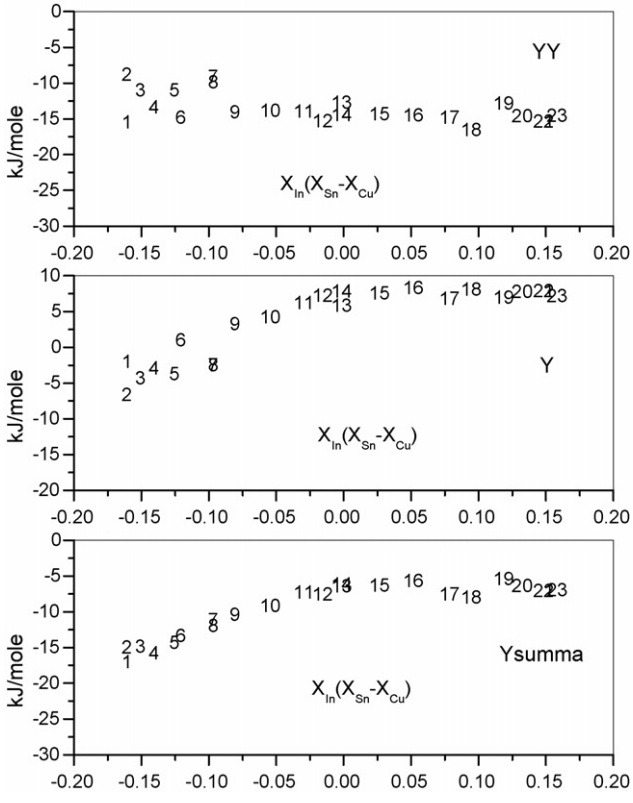

Fig. 2. Top: Y as a function of $X_{In}\cdot(X_{Sn} - X_{Cu})$ at 1373 K; middle: YY as a function of $X_{In}\cdot(X_{Sn} - X_{Cu})$ at 1373 K; bottom: Ysumma as a function of $X_{In}\cdot(X_{Sn} - X_{Cu})$ at 1373 K.

Table 4
Ternary L-parameters obtained by the multilinear regression at selected temperatures

T (K)	$-C$ (intercept) (J/mol)	L^0 (J/mol)	L^1 (J/mol)	L^2 (J/mol)	Correlation coefficient
800	−13136 (±5%)	45945 (±70%)	92019 (±70%)	−38648 (±90%)	0.669
1000	−11632 (±4%)	52377 (±40%)	76890 (±50%)	−31879 (±75%)	0.808
1273	−8630 (±3%)	55509 (±16%)	55288 (±30%)	−25980 (±40%)	0.954
1323	−7980 (±3%)	55515 (±12%)	51190 (±25%)	−25241 (±30%)	0.970
1373	−7302 (±3%)	55294 (±10%)	47169 (±25%)	−24645 (±25%)	0.979
1423	−6596 (±2%)	54950 (±10%)	43041 (±25%)	−24100 (±25%)	0.981
1473	−5864 (±2%)	54450 (±10%)	38901 (±30%)	−23665 (±30%)	0.972
$-C = -(4817 \pm 1487) - (115.0 \pm 8.9)\cdot T + (15.7 \pm 1.1)\cdot T\cdot\ln(T)$					
$L^0 = (-59473 \pm 7057) + (726.8 \pm 42.3)\cdot T - (89.0 \pm 5.1)\cdot T\cdot\ln(T)$					
$L^1 = (156840 \pm 5.2\text{E}-9) - (80 \pm 3.3\text{E}-11)\cdot T - (5.57\text{E-}11 \pm 4\text{E}-12)\cdot T\cdot\ln(T)$					
$L^2 = (-137168 \pm 8819) + (592.4 \pm 52.9)\cdot T - (70.6 \pm 6.4)\cdot T\cdot\ln(T)$					

The parameters of the $L(T)$ functions. The values behind ± are standard deviations of the statistical error.

involving no measuring error and true values for the binary parameters, only the sum of Y and YY, i.e., Ysumma, should be a smooth function of $X_{In}\cdot(X_{Sn} - X_{Cu})$ in contrast to the Y and YY versus $X_{In}\cdot(X_{Sn} - X_{Cu})$ (see the number legends in Fig. 2). This is obvious since the same value of $X_{In}\cdot(X_{Sn} - X_{Cu})$ can be obtained from different compositions. Miki and Ogawa [4,11] define the ternary interaction parameter (one only) by the slope of $(Y + YY)$ versus the corresponding X-axis. It is evident from Fig. 2 that in our case no such treatment is possible due to the non-linear dependence of Ysumma versus $X_{In}\cdot(X_{Sn} - X_{Cu})$ and multiple regressions are necessary (see Thermodynamics and solution models). We performed the regression analyses between 1273–1473 and at 1000 and 800 K. Table 4 gives the resulting regression parameter values together with their correlation coefficients. To present the correlation of the data in graphical form, the appropriate two-dimensional functions are plotted and Fig. 3 shows the measured Ysumma plotted against the calculated Ysumma, i.e Ysummacalc which is calculated from the parameters obtained from the multilinear regression (see Eq. (12)). Fig. 3 shows how, as in an ideal case, the Y-intercept nears zero and the slope is almost one. At lower and/or higher temperatures this correlation is not as strong indicating a non-ideal correlation between our measured temperature trend (values α and β, Table 3) and the temperature variation of the published binary parameters (see Eqs. (16)–(18)). The parameters obtained from the multilinear regression as a function of temperature are shown in Fig. 4. From a fit of the values between 1273 and 1473 K (measured temperature interval) to a $A + BT + CT\ln(T)$ form we observe that L^0 and L^2 have a non-linear dependence on temperature while L^1 and C are essentially linear. In addition, at 800 and 1000 K the extrapolated values coincide with individual values obtained from multilinear regression. This is a surprising result since the parameters obtained from the multilinear fitting at 800 and 1000 K possess large uncertainties (∼80%) due to these two temperatures being below the temperature range of the KEMS measurements. At 800 and 1000 K, the validity of the parameters α and β in Table 3 was not expected. The ternary L-parameters and their temperature dependence obtained by us have been compared with the values assessed by Liu [12]. Fig. 4 shows a complete mismatch.

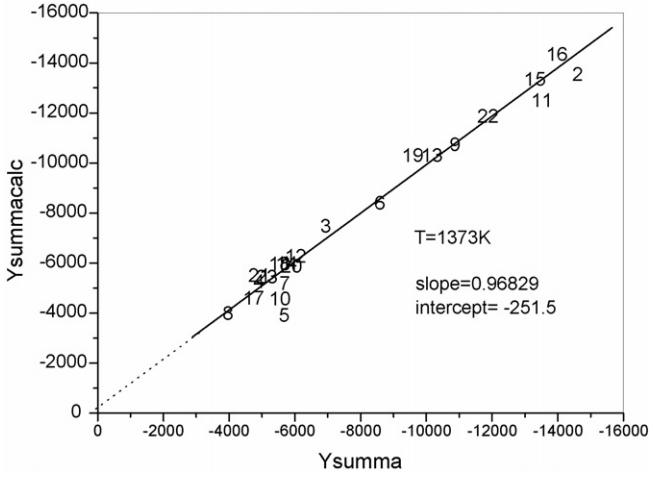

Fig. 3. The good correlation between calculated summacalc$Y$ and directly measured summa$Y$ indicates the reliability of the results at 1373 K. The correlation at 1000 K is much worse (slope = 0.8, intercept = −2400).

We believe it is instructive to compare the regression parameter C with its real physical meaning. Refs. [4,5,11] show that the regression parameter C refers to the expression (14)

$$\Delta_{vap}G^{\circ}_{Cu} - \Delta_{vap}G^{\circ}_{Sn} + RT\ \ln\left(\frac{k_{Cu}}{k_{Sn}}\right) \tag{14}$$

where $\Delta_{vap}G^{o}$ is the standard Gibbs free energy of evaporation and the k's represent the first term on the right hand side of Eq. (1), the value of which can be determined. Using the literature values for $\Delta_{vap}G^{o}$ [13] and the corresponding parameter values defined in Eq. (1), the values obtained from Eq. (14) are in good agreement with the regression parameter C in the measured temperature interval (Table 5), and is still acceptable at extrapolated temperatures. It may therefore be assumed that other regression

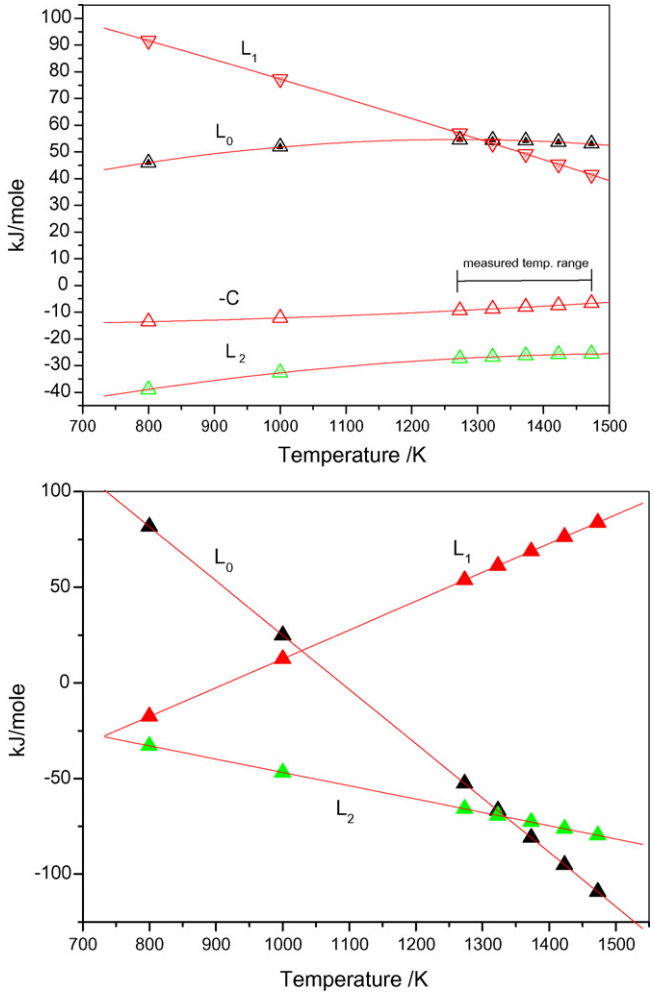

Fig. 4. Top: the Redlich–Kister ternary L-parameters as a function of temperature obtained in this work. *Bottom*: The Redlich–Kister ternary L-parameters as a function of temperature assessed by Liu [12].

parameters $L^0_{\mathrm{Cu–In–Sn}}$, $L^1_{\mathrm{Cu–In–Sn}}$, $L^2_{\mathrm{Cu–In–Sn}}$ can be considered as reliable at least between 1273 and 1473 K.

We can obtain the excess integral Gibbs energy using Eq. (7). Using Eqs. (4) and (5) and by analogy (15) the partial excess chemical potentials and/or activities of all three components can

Table 5
Values of C, obtained from the literature data and from this work, for selected temperatures

T (K)	$\frac{G^\circ_{\mathrm{vap,Cu}} - G^\circ_{\mathrm{vap,Sn}}}{\mathrm{J/mole}}$	$\frac{\Delta_{\mathrm{vap}}G^\circ + R\cdot T\cdot \ln\left(\frac{\sigma_{\mathrm{Sn}}\cdot\eta_{\mathrm{Sn}}}{\sigma_{\mathrm{Cu}}\cdot\eta_{\mathrm{Cu}}}\right)}{\mathrm{J/mole}}$	$\frac{-C}{\mathrm{J/mole}}$
800	−11210	−11946	−13130
1000	−9212	−10131	−11630
1273	−6484	−7654	−8629
1323	−5984	−7200	−7979
1373	−5484	−6746	−7300
1423	−4985	−6293	−6595
1473	−4485	−5839	−5864
$\sigma_{\mathrm{Cu}} = 3.75$ (25 eV)	Ref. [6]	$\eta_{\mathrm{Cu}} = 0.69$	
$\sigma_{\mathrm{Sn}} = 7.02$ (25 eV)		$\eta_{\mathrm{Sn}} = 0.33$	

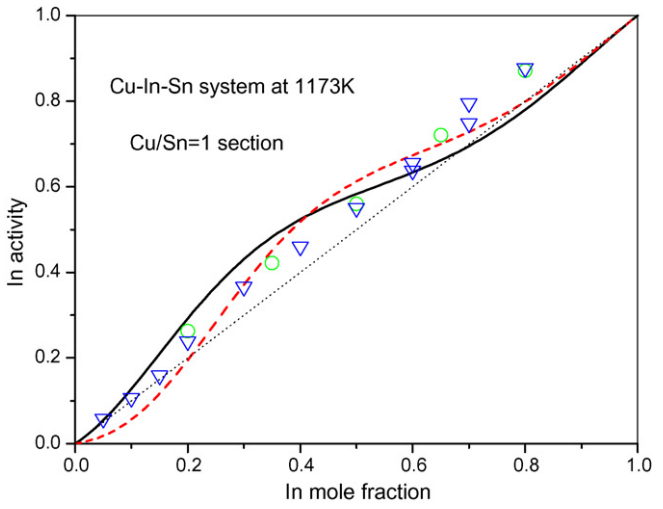

Fig. 5. The calculated (modelled) and measured activity of indium along the $X_{\mathrm{Cu}}/X_{\mathrm{Sn}} = 1$ isopleths as a function of X_{In} at 1173 K. Solid line: calculated using our ternary parameters; dashed line: calculated using Liu's ternary parameters; circles: measured data from Yamaguchi [14]; triangles: measured data, this work.

be determined.

$$\mu^{\mathrm{E}}_{\mathrm{In}} = G^{\mathrm{E}} - X_{\mathrm{Cu}}\left(\frac{\partial G^{\mathrm{E}}}{\partial X_{\mathrm{Cu}}}\right)_{X_{\mathrm{Sn}}} - X_{\mathrm{Sn}}\left(\frac{\partial G^{\mathrm{E}}}{\partial X_{\mathrm{Sn}}}\right)_{X_{\mathrm{Cu}}} \quad (15)$$

Fig. 5 shows the calculated activities for indium at the Cu/Sn = 1 section. Also shown are the activities calculated using the ternary parameters of Liu [12]. We obtained somewhat different values at lower indium mole fractions (see Fig. 5). To compare the obtained (modelled) results with measured values we performed a series of Knudsen effusion mass loss rate experiments along the Cu/Sn = 1 isopleths that give the activity of indium from $X_{\mathrm{In}} = 0.05$ to $X_{\mathrm{In}} = 0.8$ (Fig. 5). We observe a good agreement between the indium activities obtained from our own mass loss experiments and the experimental data of Yamaguchi [14]. This good agreement with the values obtained from our ternary interaction parameters is however valid only in the low mole fraction of the indium region. So far we have no explanation for this mismatch between experimental and modelled values at higher indium contents.

6. Reliability of measurements and sources of errors

The ternary interaction parameters in this work are obtained from the literature binary parameters and from the Knudsen effusion mass spectrometric measurements; the latter are relative measurements i.e., the ratio of two ion currents measured as a function of temperature. In our case, there is no need for pressure calibration and hence we expect no significant systematic error originating from calibration difficulties. A statistical error however does remain in the uncertainties of α and β in Table 3. On the contrary, the use of binary parameters introduces systematic error only and it is therefore important to use well assessed and accepted values. The following values used in this work for Cu–In and Cu–Sn binaries were taken from Ref. [12] but are

also accepted by Ref. [15]

$$L^0_{\mathrm{Cu-In}} = -41564.79 + 238.616 \cdot T - 29.827 \cdot T \cdot \ln(T)$$
$$L^1_{\mathrm{Cu-In}} = -76057.785 + 371.306 \cdot T - 44.944 \cdot T \cdot \ln(T)$$
$$L^2_{\mathrm{Cu-In}} = -42076.516 + 192.395 \cdot T - 23.281 \cdot T \cdot \ln(T) \quad (16)$$

$$L^0_{\mathrm{Cu-Sn}} = -9002.8 - 5.8381 \cdot T$$
$$L^0_{\mathrm{Cu-Sn}} = 20100.4 + 3.6366 \cdot T \quad (17)$$
$$L^2_{\mathrm{Cu-Sn}} = -10528.4$$

For an In–Sn liquid system however, there are a number of parameter sets [16–19] resulting in different excess Gibbs energy (Fig. 6). All sets are considered in our calculations but no significant differences exist in the resulting ternary L-values. This is probably due to the low contribution of the binary In–Sn to the total excess Gibbs energy of the ternary system Eq. (7). But it is noteworthy, that the best correlation of multiple regression was obtained using the binary data of Ansara [19], Eq. (18) for In–Sn. In contrast, the worst correlation is in Liu's data [12] for In–Sn, that is, Liu's G_{ex} deviates notably from the others (Fig. 6).

$$L^0_{\mathrm{In-Sn}} = -828.54 + 0.76018 \cdot T - 0.1212 \cdot T \cdot \log(T)$$
$$L^1_{\mathrm{In-Sn}} = -115.59 - 1.39997 \cdot T \quad (18)$$

Since there is a mismatch in absolute values and temperature trends between the ternary parameters obtained in this work and those assessed by Liu [12], it is necessary to outline the differences between the two approaches. The reliability of the results in our work is based on the reliability of the three sets of binary liquid parameters and the accuracy and/or reproducibility of mass spectrometric measurements. The assessment data of Liu [12] depends on the reliability of the parameter sets of all coexisting phases at temperatures below liquidus. Unfortunately, mass spectrometric measurements were made at temperatures sufficient and much beyond liquidus to provide measurable ion currents for Cu^+ and Sn^+. The thermodynamic data (ternary parameters) obtained by mass spectrometric measurements must have a reliable temperature dependence (values of α in Table 3) to be useful for computation of the liquidus surface at temperatures much lower than the temperature range of the measurements. However, we show that the temperature dependence of the regression parameter $-C$ approximates that obtained from the literature-data obtained by independent methods, and therefore it is unlikely that the temperature dependence of other L's are far from "real" values.

As an additional proof for the reliability of our L's we performed a series of measurements that give the partial heat of mixing of indium along the Cu/Sn = 1 isopleths and compare the calculated values using ternary parameters. We should note that such measurements are common in KEMS studies of alloys that typically provide partial heats of mixing with a precision of about $\pm 0.2R$, if extremely careful measurements are made. The method involves measuring the ion current of a particular element (indium in this case) in variation with temperature for

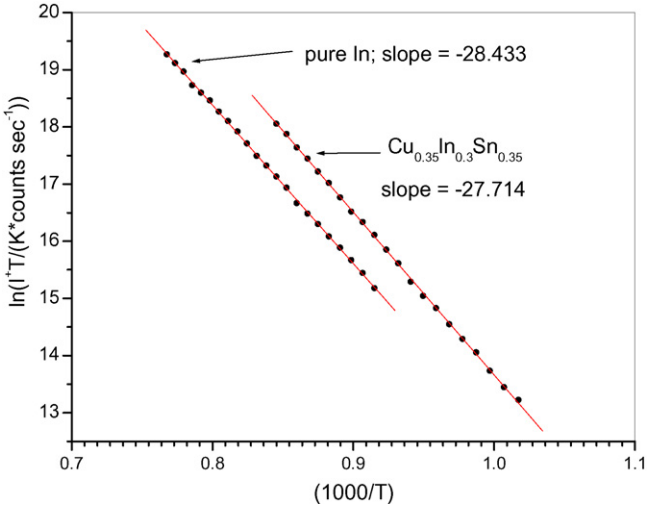

Fig. 7. Clausius–Clapeyron plot for indium in $Cu_{0.35}In_{0.30}Sn_{0.35}$ alloy and pure indium. From difference in slopes, partial heat of mixing is obtained as +5.9 kJ/mol.

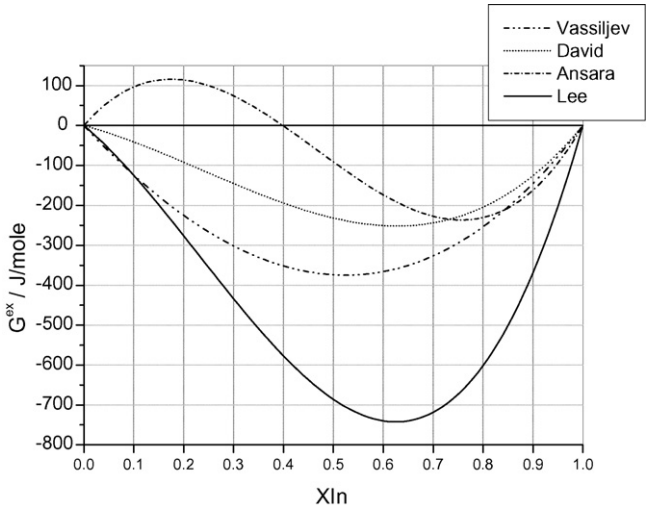

Fig. 6. Various literature data of the excess Gibbs energy of In–Sn system at 1200 K.

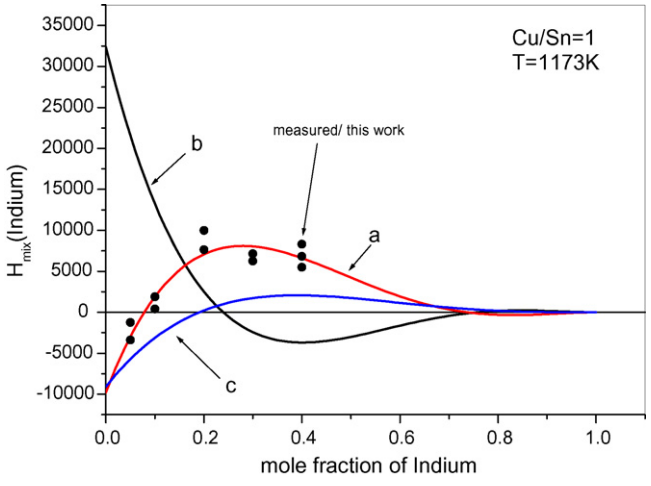

Fig. 8. Measured H_{mix} of indium compared with calculated values using: (a) our ternary parameters; (b) Liu ternary parameters; (c) binary parameters only.

a pure metal and alloy, respectively. The partial heat of mixing is then obtained from the difference in the slopes of the two Clausius–Clapeyron plots, defined as $\ln(I_{In}^{+} \cdot T)/(1/T)$, see Ref. [6]. Fig. 7 shows a typical example of this type of experiment while Fig. 8 show a comparison of the results with the calculated values. Good agreement is observed for those calculations where our ternary parameters are used for modelling.

7. Conclusions

Ternary interaction parameters for a liquid Cu–In–Sn system were obtained based on binary parameters and mass spectrometric measurements of (Cu^+/Sn^+) ion current ratio dependence on temperature. A good agreement is obtained between the indium activities determined from the measured mass loss using the Knudsen effusion mass loss technique and from the measured Cu^+ to Sn^+ intensity ratios used for the Redlich–Kister subregular solution model at values below $x_{In} < 0.5$. A good agreement also exists between the measured partial heat of mixing of indium along the Cu/Sn = 1 isopleths and the calculated one indicating that the temperature trend of our ternary Redlich–Kister L parameter values are close to "real" values. There is, however a complete mismatch, both in absolute values and temperature trends, between the ternary L-parameters obtained in this work and published values.

References

[1] H.L. Lukas, J. Weiss, E.-T. Henig, CALPHAD (1982) 229.
[2] D.W. Marquardt, J. Soc. Ind. Appl. Math. 11 (1963) 431.
[3] E. Königsberger, CALPHAD 15 (1991) 69.
[4] T. Miki, N. Ogawa, T. Nagasaka, M. Hino, Mater. Trans. 42 (2001) 732.
[5] H. Schmidt, J. Tomiska, J. Alloys Compd. 385 (2004) 126.
[6] J. Drowart, C. Chatillon, J. Hastie, D. Bonnell, Pure and Appl. Chem. IUPAC-Technical Report 77 (4), p. 683, 2005.
[7] A. Popovic, Int. J. Mass Spectros. 230 (2003) 99.
[8] G.R. Belton, R.J. Fruehan, Metall. Trans. 1 (4) (1970) 781.
[9] Y.M. Muggianu, M. Gambino, L.P. Bros, J. Chim. Phys. 72 (1975) 85.
[10] J. Valderrama-N, K.T. Jacob, Thermochem. Acta 21 (1977) 215.
[11] N. Ogawa, T. Miki, T. Nagasaka, M. Hino, Mater. Trans. 43 (2002) 3227.
[12] X.J. Liu, H.S. Liu, I. Ohnuma, R. Kainuma, K. Ishida, S. Itabashi, K. Kameda, K. Yamaguchi, J. Electron. Mater. 30 (9) (2001) 1093.
[13] IVTANTHERMO, Thermocentre of the Russian Academy of Science, CRCSeries, New York, 1993.
[14] K. Yamaguchi, private communication.
[15] Cost 531 database.
[16] B.J. Lee, C.S. Oh, J.H. Shim, J. Electron. Mater. 25 (1996) 983.
[17] V. Vassiliev, Y. Feutelais, M. Sghaier, B. Legendre, Thermochim. Acta 315 (1998) 129.
[18] N. David, K. El Aissaoui, J.M. Fiorani, J. Hertz, M. Vilasi, Thermochem. Acta 413 (2004) 127.
[19] I.N. Ansara, Unpublished result stored within the COST531 database.